OPEN

Citation: Cell Death and Disease (2014) 5, e1158; doi:10.1038/cddis.2014.114

www.nature.com/cddis

Mutation of a Nopp140 gene *dao-5* alters rDNA transcription and increases germ cell apoptosis in *C. elegans*

C-C Lee[1,4], Y-T Tsai[2,3,4,5], C-W Kao[2], L-W Lee[2], H-J Lai[2], T-H Ma[2,3], Y-S Chang[2,3], N-H Yeh[1] and SJ Lo*[,1,2]

Human diseases of impaired ribosome biogenesis resulting from disruption of rRNA biosynthesis or loss of ribosomal components are collectively described as 'ribosomopathies'. Treacher Collins syndrome (TCS), a representative human ribosomopathy with craniofacial abnormalities, is attributed to mutations in the *tcof1* gene that has a homologous gene called *nopp140*. Previous studies demonstrated that the *dao-5* (*dauer and aged animal overexpression gene 5*) of *Caenorhabditis elegans* is a member of *nopp140* gene family and plays a role in nucleogenesis in the early embryo. Here, we established a *C. elegans* model for studying Nopp140-associated ribosomopathy. A null *dao-5* mutant *ok542* with a semi-infertile phenotype showed a delay in gonadogenesis, as well as a higher incidence of germline apoptosis. These phenotypes in *dao-5*(*ok542*) are likely resulted from inefficient rDNA transcription that was observed by run-on analyses and chromatin immunoprecipitation (ChIP) assays measuring the RNA Pol I occupancy on the rDNA promoter. ChIP assays further showed that the modifications of acetylated histone 4 (H4Ac) and dimethylation at the lysine 9 of histone 3 (H3K9me2) around the rDNA promoter were altered in *dao-5* mutants compared with the N2 wild type. In addition, activated CEP-1 (a *C. elegans* p53 homolog) activity was also linked to the loss of DAO-5 in terms of the transcriptional upregulation of two CEP-1 downstream effectors, EGL-1 and CED-13. We propose that the *dao-5* mutant of *C. elegans* can be a valuable model for studying human Nopp140-associated ribosomopathy at the cellular and molecular levels.

Cell Death and Disease (2014) **5,** e1158; doi:10.1038/cddis.2014.114; published online 10 April 2014
Subject Category: Experimental Medicine

Reliable ribosome biogenesis is essential to cell growth and maintenance. Impairments in ribosome biogenesis that are caused by genetic mutations of nucleolus-associated proteins or ribosomal proteins have been described as nucleolar stress or ribosomal stress (for review, see Boulon *et al.*[1] and references therein). Recently, various human genetic diseases such as Diamond–Blackfan anemia (DBA), Schwachman–Diamond syndrome (SDS), X-linked dyskeratosis congenita (DKC), cartilage hair hypoplasia (CHH), and Treacher Collins syndrome (TCS) have been associated with impaired ribosome biogenesis and functions, and are jointly referred to as 'ribosomopathies' (for review, see Narla and Ebert[2] and references therein). Although each disease results from defects in various aspects in ribosome biogenesis, for example, the mutations found in ribosomal protein genes (DBA and SDS) or the genes encoding factors associated with ribosomal DNA (rDNA) transcription (TCS) and ribosomal RNA (rRNA) processing (DKC), respectively, the resultant diseases display distinct clinical symptoms, most of which involve bone marrow failure, skeletal, and/or craniofacial defects.[3]

Notably, the etiological mutations of human TCS are heterogeneous. Autosomal mutations in the *tcof1* gene that encodes a nucleolar protein known as Treacle provide the major link to TCS pathogenesis,[4] whereas a minority of TCS individuals with intact Treacle (8%) have recently been identified to harbor mutated POLR1D or POLR1C, the common subunits of RNA polymerase I and III.[5] Treacle has also been shown to play an important role in rDNA transcription[6] and is implicated in 2'-*O*-methylation of 18S rRNA for maturation.[7] A homolog of Treacle, Nopp140 (nucleolar phosphorylated protein of 140 kD), which has as yet no human disease associated with it, could potentially be involved in ribosomopathogenesis.

Nopp140 is a highly phosphorylated protein whose tripartite organization is highly conserved and similar to Treacle (Figure 1a). Both nucleolar proteins can bind to the rDNA chromatin and participate in rDNA transcription via their C-terminal domains, respectively.[8,9] Nopp140 was first demonstrated to be a chaperon for shuttling between the nucleolus and cytoplasm in rat liver cells.[10] Nopp140 has also

[1]Institute of Microbiology and Immunology, National Yang-Ming University, Taipei 112, Taiwan; [2]Department and Graduate Institute of Biomedical Sciences, College of Medicine, Chang Gung University, Taoyuan 333, Taiwan and [3]Molecular Medicine Research Center, College of Medicine, Chang Gung University, Taoyuan 333, Taiwan
*Corresponding author: SJ Lo, Department of Biomedical Sciences, College of Medicine, Chang Gung University, Taoyuan 333, Taiwan. Tel: +886 3 2118800, ext. 3295; Fax: +886 3 2118392; E-mail: losj@mail.cgu.edu.tw
[4]These authors contributed equally to this work.
[5]Current address: Institute of Molecular Medicine and Genetics, Georgia Regents University, Augusta, Georgia, USA
Keywords: nucleolus; ribosomopathy; Nopp140; rDNA; evolution
Abbreviations: ChIP, chromatin immunoprecipitation; Nopp140, nucleolar phosphorylated protein of 140 kD; TCS, Treacher Collins syndrome; snoRNP, small nucleolar ribonucleoprotein
Received 18.4.13; revised 17.2.14; accepted 20.2.14; Edited by Y Shi

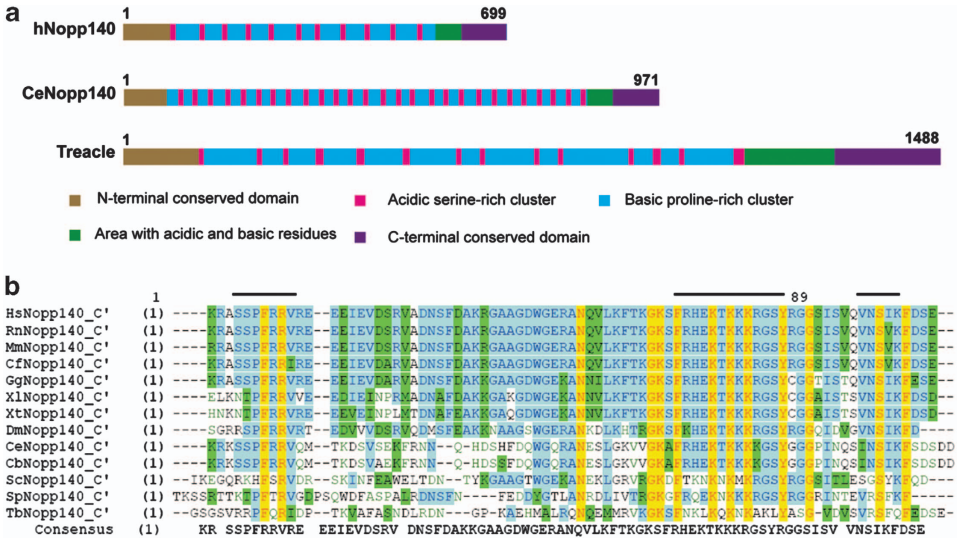

Figure 1 Protein features among human Treacle, Nopp140, and *C. elegans* DAO-5 and amino acid alignment of the C-termini. (**a**) Scheme of the tripartite features, which possess an N-terminal domain, a central acid-basic domain, and a C-terminal domain of human and *C. elegans* Nopp140, and human Treacle are shown, respectively. The explanation of each colored domain is indicated below. The number at the end of schemes indicates the total amino acid residues of each protein. (**b**) The C-terminal domain of Nopp140s is highly conserved across metazoans. The residues in yellow are identically conserved and residues in blue are highly conserved whereas the moderately conserved residues are shown in green. The highly conserved stretches of amino acid residues between *C. elegans* and humans are indicated with a line above the alignment. Hs, *Homo sapiens*; Rn, *Rattus norvegicus*; Mm, *Mus musculus*; Cf, *Canis familiaris*; Gg, *Gallus gallus*; Xl, *Xenopus laevis*; Xt, *Xenopus tropicalis*; Dm, *Drosophila melanogaster*; Ce, *Caenorhabditis elegans*; Cb, *Caenorhabditis briggsae*; Sc, *Saccharomyces cerevisiae*; Sp, *Schizosaccharomyces pombe*; Tb, *Trypanosoma brucei*

been reported to be an RNA pol II transcriptional regulator[11] and a binding target of doxorubicin,[12] an anticancer agent. Reports show that human Nopp140 (hNopp140) plays important roles in rRNA biosynthesis by interacting with the largest subunit of RNA polymerase I (Pol I) in HeLa cells.[13] In addition, hNopp140 can bind to the rDNA and α-satellite array and thus it has been proposed to function as a scaffold protein for maintaining the integrity of rDNA transcription and the nucleolar structure.[9] According to functions linked to the identified Nopp140-associated proteins, including NAP57 (Nopp140 associating protein of 57 kD), NAP65, and p80-coilin, it has been suggested that Nopp140 might also play a role in rRNA processing as a small nucleolar ribonucleoprotein (snoRNP) chaperon (for review, see He and Dimario[14] and Lo *et al.*[15] and references therein). NAP57 (also known as dyskerin) is a component of box H/ACA snoRNPs that participates in pseudouridylation of pre-rRNA.[16] Of note, mutation of the *NAP57* gene in humans leads to another important ribosomopathy disease, dyskeratosis congenita (see above). Altogether, Nopp140 is tightly associated with rRNA biosynthesis and might also be implicated in ribosomopathic etiology.

To gain insights into Nopp140-dependent ribosomopathy, an animal model has been developed. Previously, a *Drosophila* Nopp140 model showed that flies with depletions of Nopp140 exhibited *minute*-like phenotypes, including malformed wings, legs, and tergites that are phenotypes highly associated with ribosomal protein insufficiency.[17] Because of the tractability of the nematode *Caenorhabditis elegans*, including shorter life cycle, transparent body, and easy handling,[18] we used *C. elegans* as an alternative animal model for investigating Nopp140 biology. We have found that a mutant of *dao-5*, a *C. elegans* Nopp140 homolog, exhibits severe gonadal defects because of impaired rRNA synthesis.

Results

DAO-5 is a member of the Nopp140 family with a highly conserved C-terminal domain. To search for a Nopp140 homolog in the *C. elegans*, the full length of 699 residues of hNopp140 was used to BLAST Wormbase (www.wormbase.org). The highest scored hit was ORF C25A1.10 that has been annotated as *dao-5* for dauer and aged animal overexpression.[19] It encodes a protein with 971 amino acid residues that contains a high percentage of four amino acids, Lys, Ser, Ala, and Asp, comprising $>60\%$ of the total residues. Amino acid sequence analysis revealed that C25A1.10 consists of three domains similar to hNopp140, but with 15 extra repeats within the central acid-basic domain (Figure 1a). The consensus sequence of the repeat in C25A1.10 is DSSSDSSDDEAPAKKTPAKAAPKPASKKA, similar to that of hNopp140: DSSSEEEKKPPTKAVVSKATTKPPAKKAAE. As the C-termini of Nopp140s from yeasts to mammals are evolutionarily conserved, which may reflect their functional importance,[9,20] the C-termini of Nopp140s and DAO-5 were aligned to highlight the sequence conservation (Figure 1b). The sequence alignment revealed that DAO-5 shares a higher percentage of identity to mammals than to unicellular organisms. Specifically, three continuous stretches (SSPFRRV, FRHEKTKKKRGSY, and NSIKF) at the same positions are identical to hNopp140 (Figure 1b).

DAO-5 is a nucleolar protein expressed in various tissues. Previously, a panel of monoclonal antibodies was generated by Hadwiger *et al.*[21] as a toolkit for studying *C. elegans*, and one of them, the monoclonal antibody 5E9, has been demonstrated to recognize DAO-5 as a nucleolar marker. Later, Korcekova *et al.*[22] used the 5E9 monoclonal

antibody to show the importance of DAO-5 during nucleogenesis in *C. elegans* embryo. To further study the DAO-5 expression pattern in a whole worm, we generated a transgenic worm carrying an extrachromosomal array of $P_{dao\text{-}5}$*::dao-5::gfp* that expressed a fusion protein of DAO-5 with green fluorescence protein (DAO-5::GFP). The DAO-5::GFP appeared in oval- to round-shaped dots, a typical appearance of nucleoli, in various tissues including nerve ring, intestine, and hypodermis (Figure 2a). Because of the 'germline silencing' effect,[23] the transgenic worms did not express DAO-5::GFP in germ cells. We dissected gonad and intestine of transgenic animals and stained with an anti-fibrillarin (a nucleolus marker[24]) antibody. We found that the ectopically expressed DAO-5::GFP was clearly colocalized with fibrillarin in the nucleoli of the somatic gonad (sheath cells) and intestinal cells (Figure 2b), indicating that the DAO-5 is indeed localized to nucleoli. Consistently, another transgenic worm carrying an inserted transgene of $P_{pie\text{-}1}$*::ORF*$_{dao\text{-}5}$*::gfp-3′UTR*$_{dao\text{-}5}$ (designated as *cguIs13*), whose germline expressed DAO-5::GFP, also revealed its nucleolar localization (Supplementary Figure S1) as previously shown.[21]

DAO-5 forms a complex with RNA Pol I. To further test whether DAO-5 is also an RNA Pol I binding partner similar to hNopp140,[13] cell lysates from N2 worms were immunoprecipitated with anti-Pol I antibodies or a control antibody followed by western blot analyses with the anti-DAO-5 antibody 5E9. Results showed that the endogenous DAO-5 could be specifically coprecipitated with RNA Pol I (Figure 2c). Taken together, we revealed that DAO-5, which is expressed in various tissues, not only predominately localizes at nucleoli but also appears similar in character to hNopp140 by forming complexes with RNA Pol I.[13]

The association of DAO-5 with rDNA. Next, we examined whether DAO-5 also interacts with rDNA in a manner similar to hNopp140.[9] *C. elegans* rDNA is $\sim$7 kb, and the rDNA cluster is located at the right arm of chromosome I (Figure 2d).[25,26] We performed chromatin immunoprecipitation (ChIP) assays to examine the endogenous DAO-5 occupancy on rDNA clusters. DAO-5 showed specific binding to the rDNA promoter region (Figure 2d) as well as the regions within the rRNA gene body (26S rRNA) and rDNA terminator. Notably, the lysate from a deletion mutant of *dao-5*(*ok542*) obtained from the *Caenorhabditis* Genetics Center, which possesses a 1.7-kb truncation (Supplementary Figure S2), exhibits little or no enrichment compared with the wild-type counterpart, indicating that the truncated gene product cannot be recognized by the 5E9 antibody. On the other hand, compared with the significant binding to the rDNA region, the DAO-5 occupancies on the promoter regions of fibrillarin (a Pol II gene) or 5S rRNA (a Pol III gene) were relatively low and insignificant between N2 and *dao-5*(*ok542)* animals (Supplementary Figure S3), suggesting that DAO-5 specifically interacts with Pol I-dedicated rRNA genes. Consistent with the results observed by Korcekova *et al.*,[22] we further demonstrated that the association of DAO-5 with rDNA and fibrillarin not only occurs in the early embryo, but also appears to be conserved throughout the organism.

Mutants of *dao-5* display gonadal defects and produce smaller broods. To better understand the role that DAO-5 plays at the organismal level, we carried out more phenotypic analyses. Although the *dao-5*(*ok542*) homozygote animal is still viable, the fertility is significantly damaged (Figure 3a). In the wild-type *C. elegans* hermaphrodite, the germline undergoes a prominent amplification to give rise to mature oocytes.[27] Although the gonadal development of *dao-5*(*ok542*) appeared normal until the fourth larval stage (L4) (Figures 3b and c), adult worms showed delayed oogenesis and consequently underdeveloped gonads (Figures 3b and c). Importantly, the phenotypes were also observed in wild-type worms with *dao-5*(*RNAi*) knockdown (data not shown), and the semisterility phenotype of *dao-5*(*ok542*) could be rescued in *dao-5*(*ok542*); *cguIs13* worms (Figures 3a and c), indicating that the fusion protein of DAO-5::GFP is functional and the germline expression of DAO-5 is sufficient for normal germline development, in particular oogenesis, the process where germ cells give rise to mature oocytes. Besides, no notable defects were found in the spermatheca in the *dao-5(ok542)* hermaphrodites (data not shown), and this supports our conclusion that the poor fertility of *dao-5* mutants is attributed to the oogenic defect.

The *dao-5* mutant displays a higher rate of germline apoptosis. As oogenesis was compromised in *dao-5*(*ok542*) mutants, we next examined whether one of the crucial landmarks in germline development, physiological apoptosis (also known as constitutive apoptosis),[28] was also affected. To monitor germ cell death, we applied a reporter transgene, *bcIs39* [$P_{lim\text{-}7}$*::ced-1::gfp*], to visualize the dying cells.[29] In *dao-5*(*ok542)* background, there were significantly increased CED-1::GFP-labeled cells in gonads as compared with those in *bcIs39* animals (Figure 3d). Although there is no strict correlation between germ cell apoptosis culling and brood size control,[30] such an increase in germ cell apoptosis also suggests that loss of DAO-5 affects gonadal development and oogenesis.

The rDNA transcription efficacy is reduced in *dao-5*(*ok542*) mutants. As DAO-5 serves as an RNA Pol I binding partner and binds to rDNA similar to its human counterpart (see above), we sought to learn whether the loss of DAO-5 would also compromise rDNA transcription, as observed in HeLa cells.[9] We compared the *in situ* run-on activities between embryonic cell cultures from N2 and *dao-5(ok542)* animals. Based on a rationale that rDNA loci are the most actively transcribed genes in an eukaryotic cell,[31] levels of the newly synthesized pre-rRNA are reflected in the nucleolar uptake of Br-UTP after a brief pulse in cells. With a 5-min exposure of Br-UTP, there was a clear distinction in Br-UTP incorporating pattern between wild-type and *dao-5*(*ok542*) cells (Figure 4a, upper two panels), of which *dao-5(ok542)* showed lower intensity of Br-UTP signal in nucleoli. However, intensities of Br-UTP signals in a longer pulse (30 min) were similar (Figure 4a, lower two panels). To confirm whether the 30-min Br-UTP incorporation can validate the difference in the nascent rRNA level between wild-type and *dao-5(ok542)* cells, we performed a quantitative dot-blot assay of Br-UTP-containing RNA (see Materials

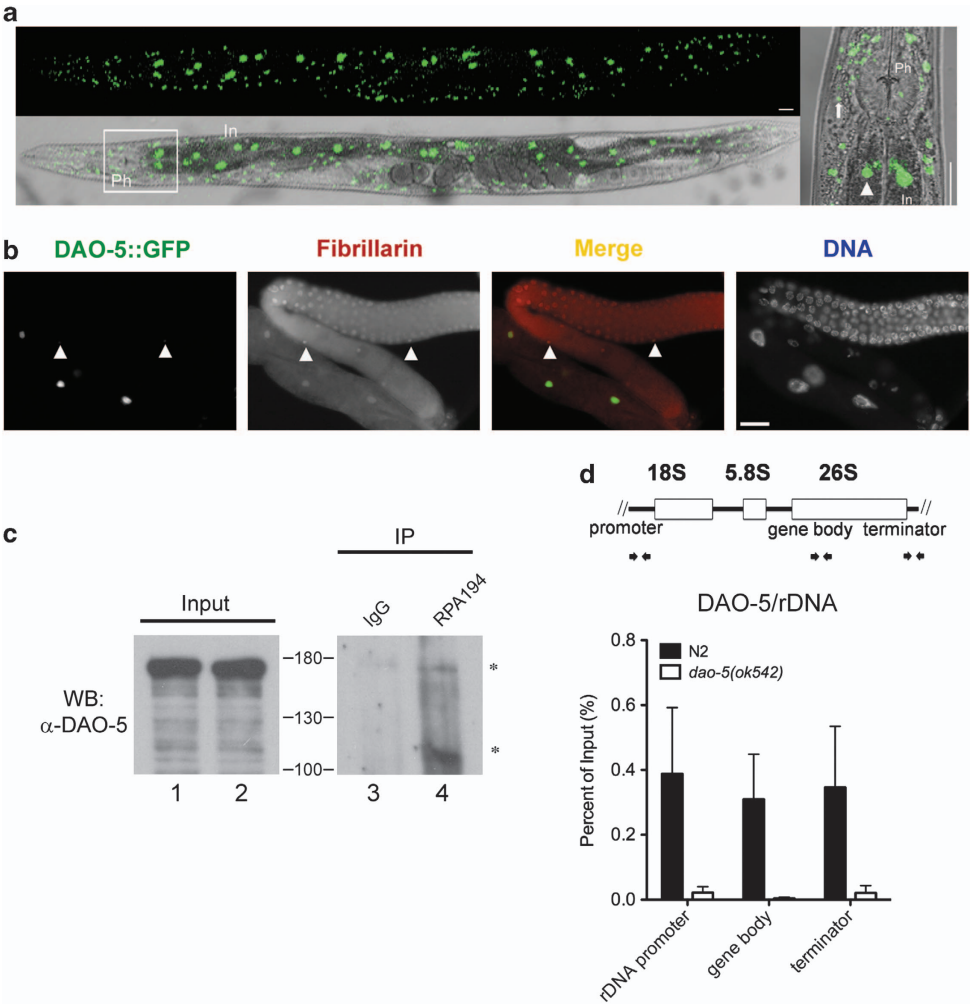

Figure 2 DAO-5 is colocalized with fibrillarin and RNA polymerase I, and binds to rDNA. (**a**) A profile of DAO-5::GFP in a transgenic worm carrying $P_{dao\text{-}5}$*::dao-5::gfp*. The head of the worm is toward the right. The confocal fluorescence image is shown in the upper panel and the superimposed image merged from the fluorescence and bright field channels is shown in the lower panel. The right panel is enlarged and turned 90-degree clock-wise from the rectangle indicated portion of worms at a low magnification. Arrowhead and arrow indicate the nucleoli in intestine cells and hypodermis cells, respectively. In, intestine; Ph, pharynx. Bar indicates 100 μm. (**b**) Ectopically expressed DAO-5::GFP by an extrachromosomal array is localized in the nucleoli of somatic gonad and intestine and colocalized with fibrillarin, a common nucleolar marker. Arrowheads indicate sheath cells and bar represents 20 μm. (**c**) Immunoprecipitation by anti-Pol I antibody (lane 4, indicated by RPA194) or a control antibody (lane 3, indicated by IgG) followed by western blot analysis probed by anti-DAO-5 antibody. Lanes 1 and 2 are total lysate input to show the presence of DAO-5 in N2 worms. Protein size markers are shown in kDa and the migration positions of DAO-5 are indicated with symbol of * at right. (**d**) Chromatin immunoprecipitation (ChIP) assay revealed that endogenous DAO-5 binds to the rDNA promoter region, gene body (26S rDNA), and terminator region. A scheme of rDNA and primers (with pairs of arrows) corresponding to the region of rDNA used for the ChIP assay are shown at top. Error bars represent S.D., $n = 3$

and Methods). As α-amanitin, the inhibitor of RNA Pol II and III, was included in the transcription mix, the signal detected on the membrane could be regarded as generally the Pol I-mediated transcriptional output. Three independent experiments showed the results of 42 to 67% in the amount of Br-UTP-labeled RNA in *dao-5*(*ok542*) cells as compared with that of N2 cells. These results suggested that nascent rRNA was lower in the *dao-5(ok542)* mutant. Moreover, the binding of RNA Pol I on the rDNA promoter was also found to be 30% less in *dao-5*(*ok542*) worms (Figure 5a). Taken together, the Br-UTP incorporation results, and the Pol I occupancy on rDNA promoter, revealed that the rDNA transcription becomes inefficient in the absence of DAO-5, suggesting that DAO-5 plays a facilitating role for maintaining the efficiency of RNA Pol I-mediated rDNA transcription in *C. elegans*.

The ablation of DAO-5 reduces active rDNA chromatin states around the promoter. As one of the most pronounced cellular activities, rDNA transcription is heavily regulated, including its chromatin status.[32] As DAO-5 readily binds the rDNA loci, we determined whether inefficient rDNA transcription in the absence of DAO-5 was the consequence of an altered chromatin state of rDNA. We conducted ChIP assays with three specific antibodies against various histone modification marks to detect the respective rDNA promoter binding abundance. First, the level of acetylated-histone H4 (H4ac), an 'active' mark, was found to be significantly

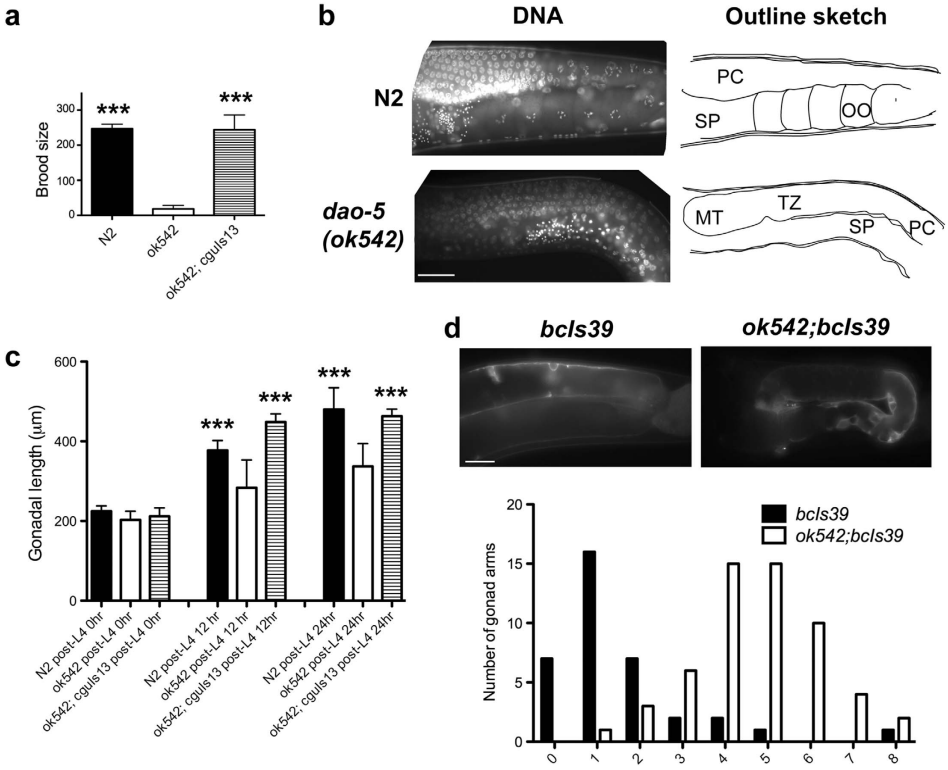

Figure 3 The absence of DAO-5 results in compromised germline development. (**a**) The brood size counting of N2, *dao-5*(*ok542*), and the rescuing transgenic (*cguIs13*) animals. Data are mean ± S.D. N2 = 247 ± 13.06 ($n = 5$); *dao-5*(*ok542*) = 18.63 ± 9.89 ($n = 8$); *dao-5*(*ok542*); *cguIs13* = 243.9 ± 42.3 ($n = 11$). Error bars represent the S.D. (**b**) The *dao-5*(*ok542*) worms exhibit a delay in gonadogenesis. N2 and *dao-5*(*ok542*) animals were fixed at the post-L4 stage at 12 h. Nuclei were highlighted with Hoechst 33342. The outlined scheme of the gonads is shown at right. MT, mitotic zone; TZ, transition zone; PC, pachytene; OO, oocytes; SP, spermetheca. (**c**) Time-course analysis showed a *dao-5*(*ok542*) hermaphrodite has a pronounced delay in germline development compared with wild-type N2 animals. The *cguIs13* animal expresses a rescuing transgene that almost fully recovers the delayed pattern observed in the *ok542* background. The average length of animals examined was as follows: for post-L4 0 h, N2 = 224.4 ± 13.47 ($n = 9$), *dao-5*(*ok542*) = 202.8 ± 21.96 ($n = 10$), and *dao-5*(*ok542*); *cguIs13* = 211.8 ± 20.91 ($n = 4$). For post-L4 12 h, N2 = 377.1 ± 24.94 ($n = 11$), *ok542* = 283.4 ± 69.88 ($n = 10$), and *dao-5*(*ok542*); *cguIs13* = 448.6 ± 20.22 ($n = 5$). For post-L4 24 h, N2 = 480.2 ± 54.3 ($n = 4$), *dao-5*(*ok542*) = 336.8 ± 57.29 ($n = 11$), *dao-5*(*ok542*); *cguIs13* = 463 ± 17.8 ($n = 7$). For post-L4 12 h, N2 *versus dao-5*(*ok542*) and *dao-5*(*ok542*); *cguIs13 versus dao-5*(*ok542*); and post-L4 24 h, N2 *versus dao-5*(*ok542*) and *dao-5*(*ok542*); *cguIs13 versus dao-5*(*ok542*), ***$P < 0.001$. (**d**) Germ cell apoptosis in worms with wild-type background (*bcls39*) or *dao-5* mutation (*dao-5*(*ok542*); *bcls39*). The reporter transgene *bcls39*, whose dying cells were decorated with CED-1::GFP, were used to facilitate the counting. Representative micrographs of the two strains are shown in the upper panel. Note that the occurrence of CED-1::GFP-surrounded cells signal in the *bcls39; ok542* is more than that of *bcls39* background. Bar represents 40 μm. Lower panel, the graphic representation of the quantitation of CED-1::GFP decorated cells counted in *bcls39* ($n = 36$) or dao-5(*ok542*); *bcls39* ($n = 56$). The X axis indicates the numbers of dying cells and the Y axis indicates the numbers of gonad arms observed

decreased in *dao-5*(*ok542*) mutants as compared with wild-type N2 animals, suggesting that DAO-5 activity is correlated to the 'activeness' of rDNA chromatin (Figure 5b). As rDNA chromatin status could be dynamic,[33,34] we next checked whether the 'inactiveness' of rDNA chromatin of *dao-5(ok542)* would be also increased correspondingly. As expected, the di-methylated histone lysine 9 of histone H3 (H3K9me2) level, an 'inactive' mark, in *dao-5*(*ok542*) was drastically increased five times compared with the low level of H3K9me2 in N2 (Figure 5c), suggesting that the absence of DAO-5 affects the 'active' level around the rDNA promoter. On the other hand, the levels of another 'inactive' mark, tri-methylated histone lysine 9 of histone H3, H3K9me3, appeared insignificantly different between N2 and *dao-5*(*ok542*) animals (Figure 5d). Interestingly, the distinct profiles of two 'inactive' histone marks, H3K9me2 and H3K9me3, around the rDNA promoter between N2 and *dao-5*(*ok542*) worms might reflect that there are distinct species of *C. elegans* rDNA (see Discussion). By and large, these ChIP results suggest that DAO-5 is important to maintain the 'active' chromatin status of the rDNA promoter to accommodate the transcribing Pol I machinery, thereby facilitating rDNA transcription.

CEP-1/p53 activity was elevated in the *dao-5(ok542)* mutant. From the data above, it could be informed that the absence of DAO-5 affects rDNA transcription accompanying the gonadal defects. To cope with malfunctioning or damaged ribosome biogenesis, a p53-responsive mechanism termed 'ribosomal stress' or 'nucleolus stress' has been long observed in mammals.[1] Previously, in *C. elegans*, several lines of evidence showed that the disrupted ribosomal biogenesis or depletion of nucleolar proteins would induce CEP-1 (the *C. elegans* p53 homolog) activity to enhance defensive or protective mechanisms in the organism.[35,36] To examine whether loss of DAO-5 would also elicit a higher CEP-1 activity, we first performed reverse transcription-quantitative PCR (RT-qPCR) to determine the

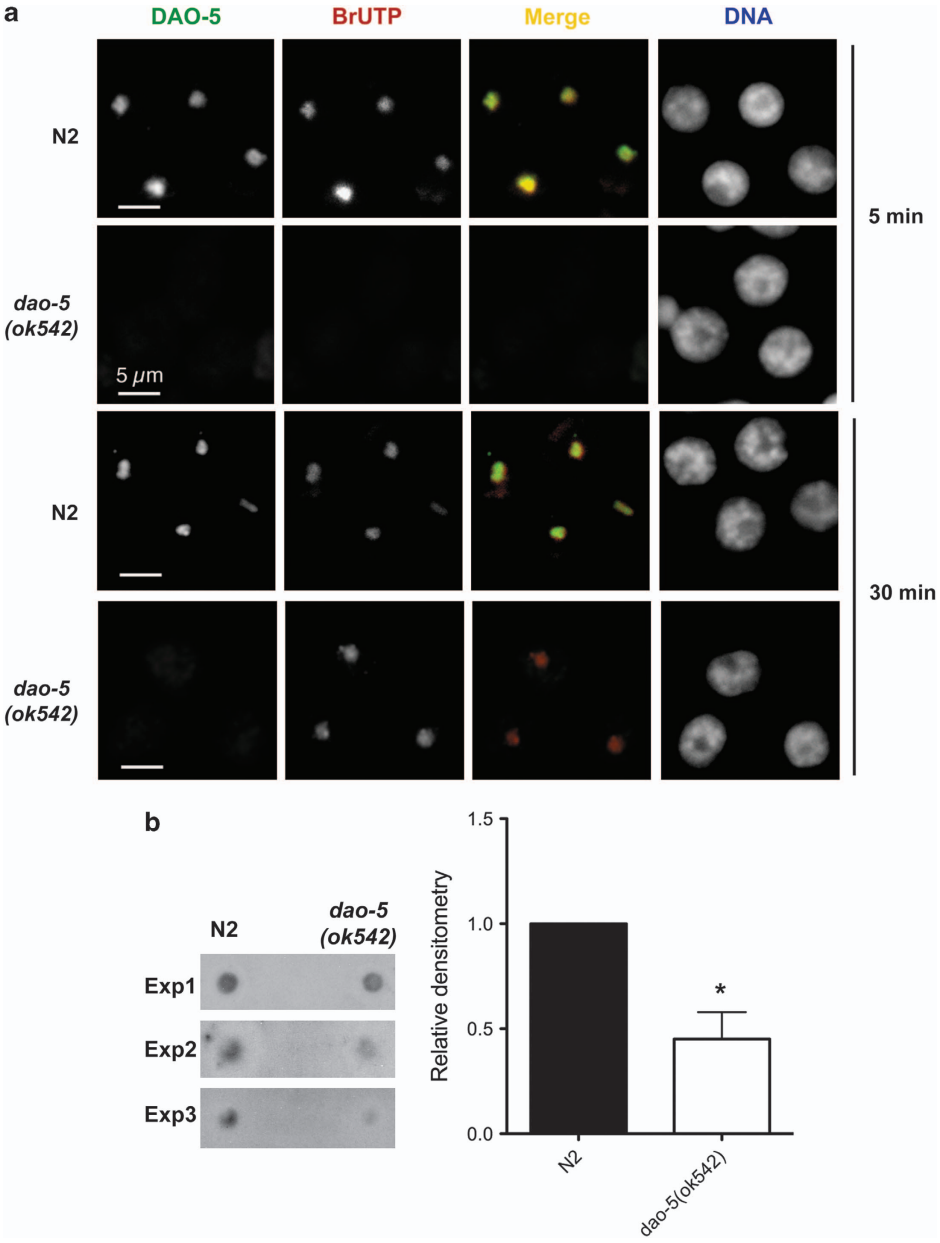

Figure 4 The absence of DAO-5 impairs the rDNA transcription efficacy. (**a**) *In situ* run-on assays were performed in the derived embryonic neuromuscular cells. Detection of Br-UTP incorporation (stained in red) is shown in the second column and the localization of DAO-5 (stained in green) is shown in the first column. The third column is merged from images of the first and the second column (shown in yellow), whereas the DNA counterstaining with Hoechst 33342 is shown in the fourth column. Note that the Hoechst 33342-negative region in the nuclei is the site of the nucleoli because the nucleolus has a high abundance of RNA but less DNA. Scale bar indicates 5 μm. (**b**) Quantitative run-on assay followed by dot-blot analysis with isolated cells from the larvae of N2 and *dao-5(ok542)* animals. The left panel shows the blots from three independent experiments and the quantitated relative densitometry data from three blots are shown in the right panel. $^*P<0.05$ in paired *t*-test

abundance of *egl-1* and *ced-13* transcripts,[37–39] both CEP-1 downstream target genes whose induction are regarded as CEP-1 activation, in N2 and *dao-5*(*ok542*) animals. The amounts of *egl-1* and *ced-13* transcripts were 2- to 6-fold higher in *dao-5*(*ok542*) worms compared with N2 (Figure 6a). Furthermore, ChIP assays also confirmed that an increased mRNA abundance was a CEP-1-mediated transcription regulation as the occupancies of CEP-1 on the *egl-1* and *ced-13* gene promoters were higher in *dao-5* background compared with that of N2 animals (Figures 6b and c). Taken together, CEP-1 activation is suggested to be responsive to the absence of DAO-5.

Discussion

The importance of DAO-5 during germline development. In addition to two reports by Hadwiger *et al.*[21] and Korcekova *et al.*,[22] in this study, we have shown that DAO-5 of

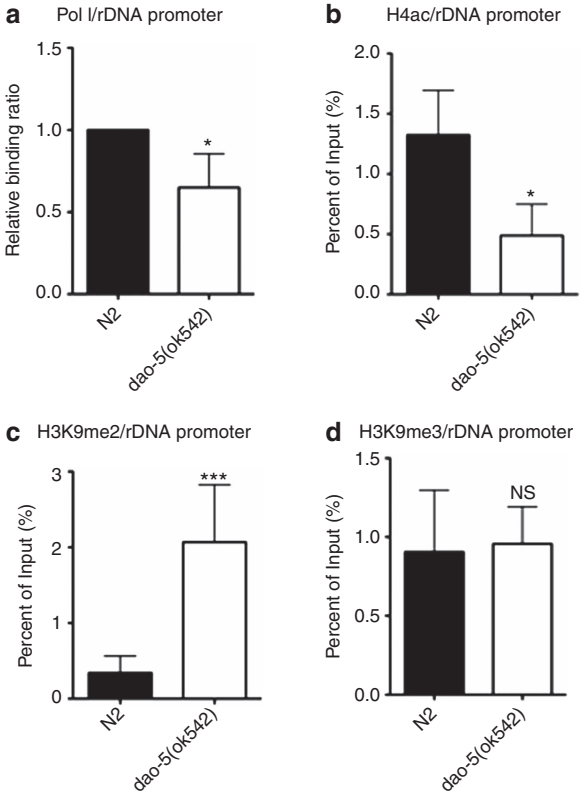

Figure 5 The absence of DAO-5 attenuates Pol I occupancy and alters the modifications of histones around the rDNA promoter. (**a**) The ChIP assays show that the occupancy of RNA Pol I in the rDNA promoter in *dao-5(ok542)* animals is weaker than that of N2. The average relative binding ratio is shown. The error bars represent S.D., $n=5$. $^{*}P<0.05$ in paired *t*-test. (**b**) The level of acetylated histone H4 (H4ac), a mark for open and actively transcribed chromatin, on rDNA promoter was found significantly decreased in *ok542* than in N2. Error bars represent the S.D., $n=4$. $^{*}P<0.05$. (**c**) The inactive mark H3K9me2 level was significantly increased in *dao-5(ok542)* compared with that in N2. Error bars represent S.D., $n=6$ in N2, $n=3$ in *dao-5(ok542)*. N2 *versus dao-5(ok542)*, $^{***}P<0.001$. (**d**) The difference in the level of inactive mark H3K9me3 between N2 and *dao-5(ok542)* was not significant. Error bars represent S.D., $n=6$ in N2, $n=4$ in *dao-5(ok542)*. No significance (NS) between N2 and *dao-5(ok542)*

C. elegans is a member of Nopp140 family, a conserved nucleolar protein across metazoans (Figures 1 and 2). DAO-5/CeNopp140 is important for sustaining germline development, particularly oogenesis. In the absence of DAO-5, worms exhibited severe defects in oogenesis together with increased germ cell apoptosis and became semi-infertile (Figure 3). DAO-5 deficiency does not cause severe effects on tissue development until the L4 stage wherein active oogenesis emerges. As an energy-demanding process that costs a large amount of proteins and RNA, oogenesis seems more sensitive to ribosome inadequacy that fails to meet the requirement during oocyte maturation. As no notable defects were found in the spermatheca in *dao-5(ok542)* hermaphrodites and males (data not shown), the fertility defect of *dao-5* mutants seems only attributed to the oogenesis. The gonadal defects observed in the absence of DAO-5 are also reminiscent of the phenotypes observed in *pro* (proximal tumor in gonad) mutants, whose ribosome production is also disrupted,[40] although their underlying mechanism may differ. Sheath cells, a specialized somatic tissue consisting of five pairs of flat cells that surround the germline, are crucial to coordinate germline development.[41] Impairments of gonadogenesis that occurred in *pro-1*, *pro-2*, and *pro-3* mutants are considered the result of the affected sheath cells in terms of lower cell number, particularly, in a nonautonomous manner.[40] We, however, are inclined to the view that the gonadal defects observed in DAO-5 deficiency are cell autonomous based on two lines of observation. First, the number of sheath cells around the gonad was not reduced in the absence of DAO-5 (data not shown). Second, the oogenic defect in a *dao-5* mutant was rescued by germline expression of DAO-5::GFP (Figures 3a and c) but not a high-copy extrachromosomal array (data not shown) that was only expressed in somatic gonadal cells including sheath cells (Figure 2b). Taken together, DAO-5 is essential for normal germline development, especially oogenesis, in a cell-autonomous manner.

Implication of DAO-5/CeNopp140 functioning to control the rDNA chromatin status. The importance of Nopp140 in rDNA transcription level has been revealed previously.[9,13] In the present study, we demonstrated that DAO-5/CeNopp140 plays a conserved role in a complex containing RNA Pol I and rDNA as shown in mammals. Loss of DAO-5 results in inefficient rDNA transcription (Figure 4) that may help explain a recent observation with decreased abundance of pre-rRNA in DmNopp140-depleted *Drosophila*.[42] Furthermore, our current study is the first demonstration that DAO-5/CeNopp140 is important to maintain the active chromatin status of rDNA (Figures 5b–d). In DAO-5-deficient worms, histone modification patterns on the rDNA promoter chromatin are altered dramatically, shifting from H4ac enriched to H3K9me2 deposition. Such a dynamic change implicates that the loss of DAO-5 renders the rDNA chromatin less active, thus compromising the rDNA transcription. On the other hand, H3K9me3 level, which is another inactive marker, does not display an increase in the absence of DAO-5. We speculate that the invariant H3K9me3 modification around rDNA may reflect the existence of the permanently dormant moiety in *C. elegans* rDNA, as revealed in mammals.[43]

How DAO-5 plays a role in controlling the rDNA transcription machinery for optimizing rRNA production is unknown. As Nopp140 serves as a nucleolar scaffold for recruiting Pol I apparatus to arrange rDNA cluster properly,[9,13] whether there is involvement of histone-modifying enzymes with DAO-5/CeNopp140, such as histone acetyltransferase (HAT) or histone demethylase (KDM), acting in concert to maintain an active rDNA chromatin status is an attractive hypothesis. For example, a histone H3K9 demethylase, PHF8, activates rDNA transcription by H3K91/2 demethylation.[44] Strikingly, a point mutation within PHF8 gene that abolishes its demethylating ability has been identified as well as a causal conjunction to another ribosomopathy, X-linked mental cleft/plate defects.[45] Therefore, the participation of histone-modifying enzymes that may potentiate in rDNA modulation of Nopp140 remains to be explored.

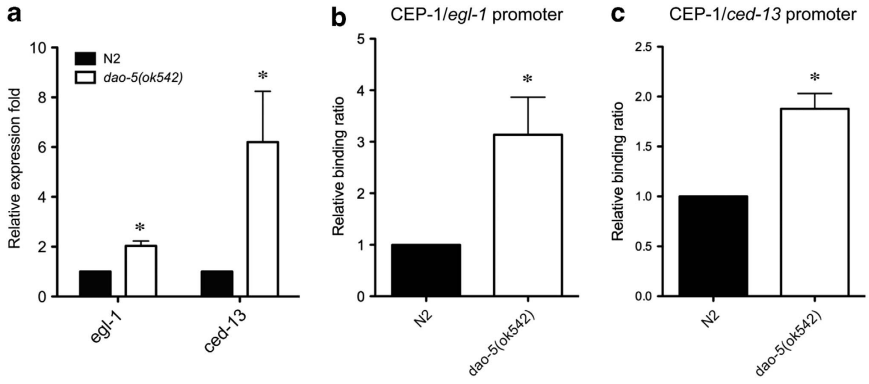

Figure 6 The CEP-1-mediated transactivation in the absence of DAO-5. (**a**) The abundance of transcripts of *egl-1* and *ced-13* (two downstream genes of *cep-1*) in N2 and *dao-5*(*ok542*) worms were compared by RT-qPCR. The average relative expression folds are shown. Error bars represent S.D, $n = 3$ in *egl-1* and $n = 4$ in *ced-13*. $^*P < 0.05$ in paired *t*-test. (**b**) The ChIP assay showed that the CEP-1 occupancies on the gene promoters of (**b**) *egl-1* or (**c**) *ced-13* was higher in *dao-5*(*ok542*) than in N2. The average binding ratios are shown. Error bars represent S.D., $n = 3$. $^*P < 0.05$ in paired *t*-test

CEP-1/p53-mediated ribosomal stress. Many studies have established p53 as the stress hub responsive to defective ribosome biogenesis (for review, see Boulon *et al.*[1]). In a TCS mouse model, p53 activation is a hallmark and is regarded as the principal cause for neuroepithelial apoptosis.[46] In this study with the *C. elegans* model, we provided evidence that both CEP-1 target genes, *egl-1* and *ced-13*, each encoding a key activator of apoptosis, would be transactivated in the absence of DAO-5 as shown in other stresses, such as genotoxic response (Figure 6).[37–39] Thus, the higher apoptotic rate found in the absence of DAO-5 (Figure 3d) seems to be conserved with the TCS murine model. Although the underlying CEP-1/p53-triggering mechanism in the absence of DAO-5/CeNopp140 remains obscure, the increase in apoptosis may serve as a protective surveillance in *C. elegans* gonad to prevent the nonqualified germ cells from giving rise to oocytes. Of note, oogenesis progression in *C. elegans* gonad, as in other species, is a G2/M transition. In mammalian contexts, however, the p53-mediated transactivation during ribosomal stress usually lead to the cell cycle arrest at the G1/S phase.[47] Interestingly, two recent studies also observed the presence of p53-mediated G2/M blockade during the induced ribosomal stress in cultured cells.[48,49] Therefore, *C. elegans* gonad may provide a platform to study the novel link of CEP-1/p53-mediated ribosomal stress with G2/M block.

In summary, results reported here have demonstrated a novel role of DAO-5/CeNopp140 in rDNA transcription and have linked its functionality with an important developmental process, oogenesis (Figure 7). The loss of DAO-5 induces ribosomal stress in terms of the activated *cep-1* transactivation to cause additional germ cell apoptosis. We thus suggest that *C. elegans* is a potentially valuable model for studying human ribosomopathy-associated diseases, given that most human genes related to ribosomopathy have been identified to have corresponding equivalents in *C. elegans*.[50] In the future, a detailed mechanism of ribosomopathy at the molecular and cellular levels might be elucidated within *C. elegans*.

Materials and Methods

Strain maintenance. All strains were maintained with standard procedures and raised at 20°C.[51] Bristol N2 was used as a wild-type animal. The *dao-5*(*ok542*) homozygote was segregated from a balanced heterozygote VC340 from *C. elegans* Gene Knockout Consortium (Oklahoma City, OK, USA). Four times of backcrossing to N2 were done before the phenotypic examination. The PCR primers used for genotyping were as follows: ok542_external_F: 5′-GATTG GTTGATTGGACCACC-3′, ok542_external_R: 5′-TGAGTTCCGACTTGTATGCG-3′; ok542_internal_F: 5′-TTTCACAAAGAAACCCGGAG-3′, ok542_internal_R: 5′-CAGTCGAGGTAGCCAATGGT-3′; and the ok542_internal_'third' primer: 5′-CTCGAGGTTACTCCAGTTGCGAAT-3′. MD701 (*bcIs39* [$P_{lim\text{-}7}$::*ced-1*::*gfp*;*lin-15*(+)]) background was used to evaluate germ cell apoptosis.[29] In the early phase of this study, N2 worms were provided by Yu-Chun Wu (National Taiwan University, Taipei, Taiwan). The other strains were then obtained from the *Caenorhabditis* Genetics Center (University of Minnesota, Twin Cities (Minneapolis and St. Paul), MN, USA).

Constructs and transgenics. Two DAO-5::GFP translational fusion transgenes with different expression cassettes were created in this study. For the $P_{dao\text{-}5}$::*dao-5*::*gfp*-expressing (DAO-5::GFP) construct, both 1498-bp *dao-5* gene promoter fragment and 3106-bp genomic DNA fragment were subsequently cloned into pPD95.75 (Addgene, Cambridge, MA, USA). The resulting transgenic line created by microinjection exists as an extrachromosomal array.[52] To express exogenous DAO-5 in the germline, a *pie-1*-driven DAO-5::GFP expression cassette ($P_{pie\text{-}1}$::*dao-5*::*gfp*::3′*UTR*$_{pie\text{-}1}$) was generated with Multisite Gateway cloning (Invitrogen, Carlsbad, CA, USA).[53] The resulting integration line (designated as *cguIs13*) was established with the microparticle bombardment technique[54] and outcrossed once to remove potentially hidden mutations. Both constructs were verified and sequenced before being subjected to transformation.

Immunoprecipitation and western blotting. The crude lysates were prepared with young adult animals in PRO-PREP lysis buffer (iNtRON, Seongnam, South Korea) supplemented with a complete protease inhibitor cocktail (Roche, Basel, Switzerland) by sonication. After centrifugation (11 000 × *g*, 4 °C, 10 min), the supernatants were collected and protein concentrations were determined by standard Bradford assay (Bio-Rad, Hercules, CA, USA). The lysate containing 2 mg of proteins was used to incubate with 4 μg of RPA194 antibody (sc-28714, Santa Cruz, Dallas, TX, USA) for 1–2 h at 4°C. The resulting immunocomplex was bound and precipitated with 50 μl protein A/G plus agarose beads (Santa Cruz) for 1 h. The beads were washed three times with NET buffer (50 mM Tris HCl, pH 7.5, 5 mM EDTA, 150 mM NaCl, 0.5% NP-40) and boiled in Laemmli sample buffer for 10 min. After 10 min of centrifugation (12 000 × *g*, 4°C), lysate suspensions of the respective sample were analyzed in 8% SDS-PAGE. Proteins were transferred to a PVDF membrane and the resulting blots were detected with the primary antibodies as indicated. The DAO-5-specific monoclonal antibody 5E9 (Developmental Studies Hybridoma Bank, Iowa City, IA, USA)[21]was used in 5–10 times

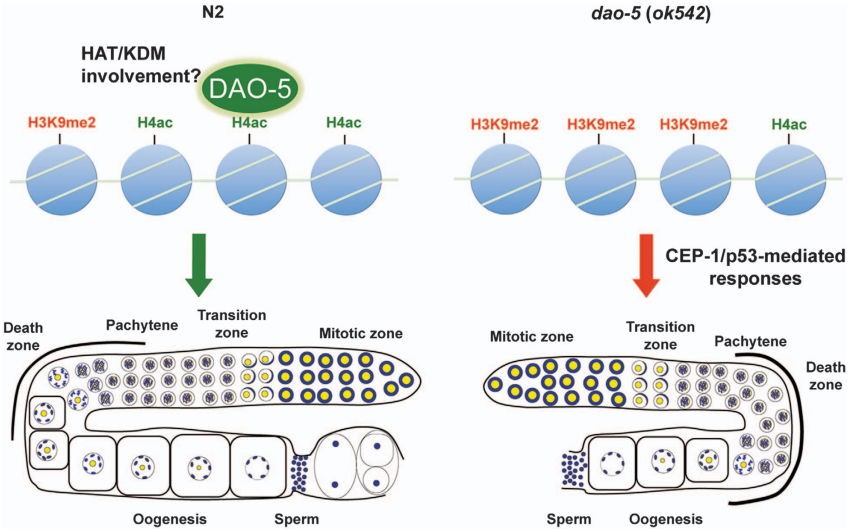

Figure 7 A working model of DAO-5 regulation in oogenesis. In the wild-type animal (N2), DAO-5 maintains the epigenetically active rDNA chromatin to facilitate rDNA transcription and sustain germline development (left scheme). Once DAO-5 is absent, rDNA transcription is hampered as rDNA becomes inaccessible because of H3K9me2 enrichment and reduced H4ac modification on nucleosomes that thereby results in alteration of rRNA synthesis and subsequently induces CEP-1-mediated ribosomal stress in terms of the increased germ cell apoptosis and impairment of oogenesis (right scheme). HAT, histone acetyltransferase; KDM, histone demethylase

dilution with 5% skim milk/PBST (0.5% Tween-20). The blots were developed and detected with chemiluminescence ECL kit (T-Pro Biotechnologies, New Taipei City, Taiwan).

Immunostaining, image acquisition, and quantitative image analyses. The global DAO-5::GFP expression pattern (Figure 2a) was acquired with a Zeiss LSM 510 Meta confocal microscope (Jena, Germany). To facilitate immunostaining, gonads were protruded by decapitating 1-day-old adult animals with 25-gauge needles and fixed with 1% formaldehyde. The fixed gonads (attached to the carcasses) were preincubated with 0.1% BSA/PBST and then stained with the anti-fibrillarin (1 : 500; Novus Biologicals, NB300-269, Littleton, CO, USA) and secondary antibody conjugated Alexa 594 (1 : 1000; Molecular Probes, Eugene, OR, USA). Images were captured with a microscope (Leica DM2500, Wetzlar, Germany) coupled with CoolSNAP K4 CCD (Photometrics, Tucson, AZ, USA) and MetaMorph software (MDS Analytical Technologies, Sunnyvale, CA, USA). For monitoring gonadal extension, the animals at their corresponding stages were collected and stored in 1 × MRWB (80 mM KCl, 20 mM NaCl, 10 mM disodium EGTA, 5 mM spermidine, 15 mM PIPES, pH 7.4, 25% methanol, 1.6% formaldehyde) at − 80°C until staining. The fixed animals were stained with Hoechst 33342 (Molecular Probes) to highlight nuclear DNA. As the gonadal tissues are mainly composed of the morphologically distinct nuclei, the overall outline and length of the developing gonads could be determined with microphotography. Images were acquired as described above and analyzed with Metamorph.

Apoptosis assessment. The reporter strain *bcIs39* $P_{lim\text{-}7}$*::ced-1::gfp*; *lin-15*(+)] was used to generate *bcIs39;ok542* to facilitate the counting of dying germ cells.[29] Living animals (~24 h post L4 stage) were mounted and anesthetized on agar pads and examined with microscopy as described above.

***In situ* and quantitative run-on assay (Br-UTP incorporation).** Procedures for conducting primary culture of *C. elegans* embryonic cells were adopted from Strange *et al.*[55] In brief, the *C. elegans* embryos were collected by hypochlorite lysis of gravid worms, and then treated with chitinase (2 U/ml, Sigma-Aldrich, St. Louis, MO, USA) at room temperature for 20 min to remove the eggshell. Following gentle trituration through a plastic 1-ml pipet tip and filtration through a 5-μm Durapore filter, the dissociated single cells were cultured in L-15 medium supplemented with 10% (v/v) heat-inactivated fetal bovine serum (Gibco, Gaithersburg, MD, USA), 50 U/ml penicillin, and 50 mg/ml streptomycin (Sigma-Aldrich) on glass coverslips coated with peanut lectin (Sigma-Aldrich) at 24°C in a humidified atmosphere. The attached cells were subjected to *in situ* transcription assay after 1 day of settlement.

In situ run-on assays were performed as described previously,[9,13] with few modifications. Briefly, cells were permeabilized by ice-cold digitonin (150 μg/ml; Sigma-Aldrich) and were incubated with 1 × transcription PB buffer (22 mM NaCl, 1 mM $MgCl_2$, 8 mM KCl, 11 mM K_2HPO_4, 100 mM CH_3COOK, 1 mM ATP, 1 mM DTT) containing NTPs mixture (Roche) and 0.2 mM Br-UTP (Sigma-Aldrich). The run-on transcription was carried out at 24°C for the indicated pulsing time (5 or 30 min), and terminated by rinsing the coverslips in ice-cold PBS. The nascent RNAs labeled by Br-UTP were visualized by immunofluorescence staining with anti-BrdU antibody conjugated with Alexa Fluor 594 (Molecular Probes) and DAO-5 was stained with a rabbit polyclonal antibody CSK-14.

To quantify the Br-UTP incorporation, isolated larval cells from N2 and *dao-5(ok542)* animals were used as described by Zhang *et al.*[56] Briefly, ~100 μl packed L4 larvae (precleared of bacteria by staying in egg buffer (118 mM NaCl, 48 mM KCl, 2 mM $CaCl_2$, 2 mM $MgCl_2$, 25 mM HEPES, pH 7.3) for 1 h) were treated with 600–800 μl SDS-DTT solution to disrupt cuticle, and the subsequent digestion with ~300 μl of pronase (15 mg/ml, Sigma-Aldrich), combined with mechanical disruption (200–250 strokes with a 200 μl tip) to release cells. After the debris was settled down, the floating dissociated cells were collected and examined under an inverted microscope (Olympus IX-71, Tokyo, Japan). The cells were pelleted and resuspended in 90 μl PB buffer supplemented with digitonin (150 μg/ml), α-amanitin (5 μg/ml), and RNase OUT (400 U/ml, Invitrogen) for preincubation at room temperature for 10 min. Following preincubation, 10 μl of 10X transcription mix with Br-UTP was added. After the 30-min pulsing period, the run-on reactions were terminated with adding 1 ml Trizol reagent (Invitrogen). RNAs were extracted with Trizol purification according to the manufacturer's instruction and resuspended in 20 μl of water.

Next, 2 μl of the total extracted RNAs (namely the run-on products) were applied onto a nylon membrane (GeneScreen Plus, PerkinElmer, Boston, MA, USA), UV cross-linked (Spectroline, Westbury, NY, USA), and then subjected to immunodetection. Br-UTP incorporated RNAs were detected with a sheep anti-BrdU antibody (1 : 1500, ab1893; Abcam, Cambridge, UK) and rabbit anti-sheep secondary antibody (1 : 3500) in 1% skim milk in TBST (0.5% Tween-20). The signals were developed and detected with chemiluminescence ECL kit (T-Pro Biotechnologies). The integrated intensities of dot blots were measured with MetaMorph software and calibrated with actin mRNA level (determined by RT-qPCR).

Chromatin immunoprecipitation. ChIP assays were performed using animals at L4 stage of the respective genotypes as previously described.[57] Briefly,

chromatin lysates were prepared from 1% formaldehyde-crosslinked animals and then sonicated to shear the chromatin DNA to a length of 500–800 bp. For determining DAO-5 occupancy, 50 μl supernatant of 5E9 hybridoma culture was used for each ChIP to incubate with the chromatin lysate (1 mg proteins). For ChIP assays with epigenetic marks, 2 μg of different antibodies, anti-H4ac (06–598, Millipore, Billerica, MA, USA), anti-H3K9me2 (ab1220, Abcam), or anti-H3K9me3 (ab8898, Abcam), were added into the lysate solution. For probing Pol I occupancy, 4 or 8 μg of anti-RPA194 antibodies (sc-28714, Santa Cruz) were coincubated with lysate. The protein A/G beads (sc-2003, Santa Cruz) were used as a precipitant of the immunocomplex. The chromatin immunoprecipitates were washed, de-crosslinked, and recovered. The abundance of genes was detected by quantitative PCR with SsoFast EvaGreen Supermix and iQ5 cycler (Bio-Rad). Oligonucleotides used in this study were as follows:

rDNA promoter: F 5′-GTGTTGGTGATGGTAGTGTGTG-3′ (587–608) and R 5′-CGGCGCAATGATATAAAGAACTCG-3′ (694–717);

26S gene body: F 5′-GGAGTGCTTGTCTACTGCGAG-3′ (4381–4401) and R 5′-CCTCTGCACAGTCACAAGTG-3′ (4531);

rDNA terminator: F 5′-TTTCCTTTTCCTACACTCATGTC-3′ (1–23) and R 5′-CCCTTCACCAGCCTCTGAAT-3′ (190–209);

fib-1 promoter: F 5′-AGATCGACTGGAGCGTGATT-3′ and R 5′-GGGAGAGCC GAGTAAGATTG-3′

5S rRNA gene promoter: F 5′-CGAGGTCTACGATCGGCAAC-3′ R 5′-GTCTAT GGACAAGTCCCATG-3′

egl-1 promoter: F 5′-ACACTTCAAGAGCTATGAGTTTGTC-3′ and R CGAACGT TTTCGAAACGG-3′;

ced-13 promoter: F 5′-GTTTCTGTCCGCCTTCCTT-3′ and R 5′-GTCGG TTATCGGTGAAACTGTA-3′.

Reverse transcription and quantitative PCR. The total RNAs of the indicated staged worms were extracted with Trizol (Invitrogen). The integrity of the RNA was inspected by 1% agarose gel analysis and the concentrations of the RNAs were determined with Nanovue (GE Healthcare, Uppsala, Sweden). Then, 1 μg of the total RNA was converted into cDNA with iScript cDNA synthesis kit (Bio-Rad). qPCR was performed with SsoFast EvaGreen Supermix in iQ5 cycler (Bio-Rad) following the standard protocol:

egl-1_coding region: F TACTCCTCGTCTCAGGACTT-3′ and R CATCGAAGT CATCGCACAT-3′;

ced-13_coding region: F 5′-TGATGTCGTACAAGCGTGAT-3′ and R 5′-AAAAA ACACGACGAACAATGCTGG-3′;

actin: F 5′-TCGGTATGGGACAGAAGGAC-3′ and R 5′-CATCCCAGTTGGTGA CGATA-3′.

Conflict of Interest

The authors declare no conflict of interest.

Acknowledgements. We thank *Caenorhabditis* Genetics Center (University of Minnesota), *C. elegans* Gene Knockout Consortium (University of British Columbia), and Yi-Chun Wu (National Taiwan University) for providing various strains of worms. We thank Scott C Schuyler (Chang Gung University) for critical reading and English editing of the manuscript. We also thank the microscope core facility of MMRC at Chang Gung University for providing the services and Yung-Hsiang Yi (Chang Gung University) for consulting on the dot-blot quantitation. This work was supported by grants (EMRPD18031, EMRPD190071, and EMRPD1A0431) from the Ministry of Education and (CMRPD160011-3) from the Chang Gung Memorial Hospital to SJL.

1. Boulon S, Westman BJ, Hutten S, Boisvert FM, Lamond AI. The nucleolus under stress. *Mol Cell* 2010; **40**: 216–227.
2. Narla A, Ebert BL. Ribosomopathies: human disorders of ribosome dysfunction. *Blood* 2010; **115**: 3196–3205.
3. Khan S, Pereira J, Darbyshire PJ, Holding S, Dore PC, Sewell WA *et al.* Do ribosomopathies explain some cases of common variable immunodeficiency? *Clin Exp Immuno* 2011; **163**: 96–103.
4. Dixon MJ. Treacher Collins syndrome. *Hum Mol Genet* 1996; **5**: 1391–1396.
5. Dauwerse JG, Dixon J, Seland S, Ruivenkamp CA, van Haeringen A, Hoefsloot LH *et al.* Mutations in genes encoding subunits of RNA polymerases I and III cause Treacher Collins syndrome. *Nat Genet* 2011; **43**: 20–22.
6. Valdez BC, Henning D, So RB, Dixon J, Dixon MJ. The Treacher Collins syndrome (TCOF1) gene product is involved in ribosomal DNA gene transcription by interacting with upstream binding factor. *Proc Natl Acad Sci USA* 2004; **101**: 10709–10714.
7. Gonzales B, Henning D, So RB, Dixon J, Dixon MJ, Valdez BC. The Treacher Collins syndrome (TCOF1) gene product is involved in pre-rRNA methylation. *Hum Mol Genet* 2005; **14**: 2035–2043.
8. Lin CI, Yeh NH. Treacle recruits RNA polymerase I complex to the nucleolus that is independent of UBF. *Biochem Biophys Res Commun* 2009; **386**: 396–401.
9. Tsai YT, Lin CI, Chen HK, Lee KM, Hsu CY, Yang SJ *et al.* Chromatin tethering effects of hNopp140 are involved in the spatial organization of nucleolus and the rRNA gene transcription. *J Biomedi Sci* 2008; **15**: 471–486.
10. Meier UT, Blobel G. Nopp140 shuttles on tracks between nucleolus and cytoplasm. *Cell* 1992; **70**: 127–138.
11. Lee YM, Miau LH, Chang CJ, Lee SC. Transcriptional induction of the alpha-1 acid glycoprotein (AGP) gene by synergistic interaction of two alternative activator forms of AGP/enhancer-binding protein (C/EBP beta) and NF-kappaB or Nopp140. *Mol Cell Biol* 1996; **16**: 4257–4263.
12. Jin Y, Yu J, Yu YG. Identification of hNopp140 as a binding partner for doxorubicin with a phage display cloning method. *Chem Biol* 2002; **9**: 157–162.
13. Chen HK, Pai CY, Huang JY, Yeh NH. Human Nopp140, which interacts with RNA polymerase I: implications for rRNA gene transcription and nucleolar structural organization. *Mol Cell Biol* 1999; **19**: 8536–8546.
14. He F, Dimario P. Structure and function of Nopp140 and Treacle. *In:* Olson MOJ (ed). *The Nucleolus (Protein Reviews)*. Springer: Heidelberg, Germany, 2011, pp 253–278.
15. Lo SJ, Lee CC, Lai HJ. The nucleolus: reviewing oldies to have new understandings. *Cell Res* 2006; **16**: 530–538.
16. Meier UT. The many facets of H/ACA ribonucleoproteins. *Chromosoma* 2005; **114**: 1–14.
17. Cui Z, DiMario PJ. RNAi knockdown of Nopp140 induces Minute-like phenotypes in Drosophila. *Mol Biol Cell* 2007; **18**: 2179–2191.
18. Ankeny RA. The natural history of *Caenorhabditis elegans* research. *Nat Rev Genet* 2001; **2**: 474–479.
19. Yu H, Larsen PL. DAF-16-dependent and independent expression targets of DAF-2 insulin receptor-like pathway in *Caenorhabditis elegans* include FKBPs. *J Mol Biol* 2001; **314**: 1017–1028.
20. Meier UT. Comparison of the rat nucleolar protein nopp140 with its yeast homolog SRP40. Differential phosphorylation in vertebrates and yeast. *J Biol Chem* 1996; **271**: 19376–19384.
21. Hadwiger G, Dour S, Arur S, Fox P, Nonet ML. A monoclonal antibody toolkit for *C. elegans*. *PLoS One* 2010; **5**: e10161.
22. Korcekova D, Gombitova A, Raska I, Cmarko D, Lanctot C. Nucleologenesis in the *Caenorhabditis elegans* embryo. *PLoS One* 2012; **7**: e40290.
23. Kelly WG, Fire A. Chromatin silencing and the maintenance of a functional germline in *Caenorhabditis elegans*. *Development* 1998; **125**: 2451–2456.
24. Meier UT, Blobel G. A nuclear localization signal binding protein in the nucleolus. *J Cell Biol* 1990; **111**(6 Pt 1): 2235–2245.
25. C. elegans Sequencing Consortium. Genome sequence of the nematode *C. elegans*: a platform for investigating biology. *Science* 1998; **282**: 2012–2018.
26. Ellis RE, Sulston JE, Coulson AR. The rDNA of *C. elegans*: sequence and structure. *Nuc Acid Res* 1986; **14**: 2345–2364.
27. Hubbard EJ, Greenstein D. Introduction to the germ line. *WormBook* 2005; 1–4.
28. Gumienny TL, Lambie E, Hartwieg E, Horvitz HR, Hengartner MO. Genetic control of programmed cell death in the Caenorhabditis elegans hermaphrodite germline. *Development* 1999; **126**: 1011–1022.
29. Zhou Z, Hartwieg E, Horvitz HR. CED-1 is a transmembrane receptor that mediates cell corpse engulfment in *C. elegans*. *Cell* 2001; **104**: 43–56.
30. Boag PR, Nakamura A, Blackwell TK. A conserved RNA-protein complex component involved in physiological germline apoptosis regulation in *C. elegans*. *Development* 2005; **132**: 4975–4986.
31. Lucchini R, Sogo JM. Replication of transcriptionally active chromatin. *Nature* 1995; **374**: 276–280.
32. Goodfellow SJ, Zomerdijk JC. Basic mechanisms in RNA polymerase I transcription of the ribosomal RNA genes. *Subcell Biochem* 2012; **61**: 211–236.
33. Murayama A, Ohmori K, Fujimura A, Minami H, Yasuzawa-Tanaka K, Kuroda T *et al.* Epigenetic control of rDNA loci in response to intracellular energy status. *Cell* 2008; **133**: 627–639.
34. Sanij E, Hannan RD. The role of UBF in regulating the structure and dynamics of transcriptionally active rDNA chromatin. *Epigenetics* 2009; **4**: 374–382.
35. Fuhrman LE, Goel AK, Smith J, Shianna KV, Aballay A. Nucleolar proteins suppress Caenorhabditis elegans innate immunity by inhibiting p53/CEP-1. *PLoS Genet* 2009; **5**: e1000657.
36. Leung CK, Empinado H, Choe KP. Depletion of a nucleolar protein activates xenobiotic detoxification genes in Caenorhabditis elegans via Nrf /SKN-1 and p53/CEP-1. *Free Radic Biol Med* 2012; **52**: 937–950.
37. Schumacher B, Schertel C, Wittenburg N, Tuck S, Mitani S, Gartner A *et al.* C. elegans ced-13 can promote apoptosis and is induced in response to DNA damage. *Cell Death Differ* 2005; **12**: 153–161.
38. Nehme R, Conradt B. egl-1: a key activator of apoptotic cell death in C. elegans. *Oncogene* 2008; **27**(Suppl 1): S30–S40.

39. Jolliffe AK, Derry WB. The TP53 signaling network in mammals and worms. *Brief Funct Genomics* 2012; **12**: 129–141.
40. Voutev R, Killian DJ, Ahn JH, Hubbard EJ. Alterations in ribosome biogenesis cause specific defects in *C. elegans* hermaphrodite gonadogenesis. *Dev Biol* 2006; **298**: 45–58.
41. Killian DJ, Hubbard EJ. *Caenorhabditis elegans* germline patterning requires coordinated development of the somatic gonadal sheath and the germ line. *Dev Biol* 2005; **279**: 322–335.
42. Neumuller RA, Gross T, Samsonova AA, Vinayagam A, Buckner M, Founk K *et al.* Conserved regulators of nucleolar size revealed by global phenotypic analyses. *Sci Signal* 2013; **6**: ra70.
43. Santoro R. The epigenetics of the nucleolus: structure and function of active and silent ribosomal RNA genes. *Nucleolus* 2011; **15**: 57–82.
44. Feng W, Yonezawa M, Ye J, Jenuwein T, Grummt I. PHF8 activates transcription of rRNA genes through H3K4me3 binding and H3K9me1/2 demethylation. *Nat Struct Mol Biol* 2010; **17**: 445–450.
45. Koivisto AM, Ala-Mello S, Lemmela S, Komu HA, Rautio J, Jarvela I. Screening of mutations in the PHF8 gene and identification of a novel mutation in a Finnish family with XLMR and cleft lip/cleft palate. *Clin Genet* 2007; **72**: 145–149.
46. Jones NC, Lynn ML, Gaudenz K, Sakai D, Aoto K, Rey JP *et al.* Prevention of the neurocristopathy Treacher Collins syndrome through inhibition of p53 function. *Nat Med* 2008; **14**: 125–133.
47. Zhang Y, Lu H. Signaling to p53: ribosomal proteins find their way. *Cancer Cell* 2009; **16**: 369–377.
48. Fumagalli S, Ivanenkov VV, Teng T, Thomas G. Suprainduction of p53 by disruption of 40S and 60S ribosome biogenesis leads to the activation of a novel G2/M checkpoint. *Genes Dev* 2012; **26**: 1028–1040.
49. Ma H, Pederson T. The nucleolus stress response is coupled to an ATR-Chk1-mediated G2 arrest. *Mol Biol Cell* 2013; **24**: 1334–1342.
50. Lee LW, Lee CC, Huang CR, Lo SJ. The nucleolus of *Caenorhabditis elegans*. *J Biomed Biotechnol* 2012; **2012**: 601274.
51. Brenner S. The genetics of *Caenorhabditis elegans*. *Genetics* 1974; **77**: 71–94.
52. Mello C, Fire A. DNA transformation. *Methods Cell Biol* 1995; **48**: 451–482.
53. Merritt C, Seydoux G. Transgenic solutions for the germline. *WormBook* 2010; 1–21.
54. Praitis V, Casey E, Collar D, Austin J. Creation of low-copy integrated transgenic lines in *Caenorhabditis elegans*. *Genetics* 2001; **157**: 1217–1226.
55. Strange K, Christensen M, Morrison R. Primary culture of *Caenorhabditis elegans* developing embryo cells for electrophysiological, cell biological and molecular studies. *Nat Protoc* 2007; **2**: 1003–1012.
56. Zhang S, Banerjee D, Kuhn JR. Isolation and culture of larval cells from C. elegans. *PLoS One* 2011; **6**: e19505.
57. Mukhopadhyay A, Deplancke B, Walhout AJ, Tissenbaum HA. Chromatin immunoprecipitation (ChIP) coupled to detection by quantitative real-time PCR to study transcription factor binding to DNA in *Caenorhabditis elegans*. *Nat Protoc* 2008; **3**: 698–709.

Supplementary Information accompanies this paper on Cell Death and Disease website (http://www.nature.com/cddis)